Spatio-Temporal Behavior of Bistable Density Transition in Magnetized Plasma

Shinohara, Shunjiro
Department of Energy Engineering Science, Kyushu University

Sugimori, Katsuhisa
Department of Advanced Energy Engineering Science, Graduate student, Kyushu University

Nakamura, Yasushi
Department of Advanced Energy Engineering Science, Graduate student, Kyushu University

Yagi, Masatoshi
Research Institute for Applied Mechanics, Kyushu University

https://doi.org/10.15017/14551

出版情報：九州大学大学院総合理工学報告. 27 (4), pp.355-360, 2006-03. 九州大学大学院総合理工学府
バージョン：
権利関係：

九州大学大学院総合理工学報告
第27巻 第4号 355-360頁 平成18年3月

Engineering Sciences Report, Kyushu University
Vol.27, No.4 pp.355-360, MAR. 2006

Spatio-Temporal Behavior of Bistable Density Transition in Magnetized Plasma

Shunjiro SHINOHARA*1,† Katsuhisa SUGIMORI*2
Yasushi NAKAMURA*3 and Masatoshi YAGI*4
†E-mail of corresponding author: *sinohara@aees.kyushu-u.ac.jp*

(Received January 31, 2006)

Self-excited bistable transition phenomena have been investigated by voltage biasing to an inserted electrode of a radio frequency (rf)-produced, magnetized plasma. Spatio-temporal behaviors of global, density transitions and back ones between two states (flip-flop pattern) have been measured, as to the ion saturation current I_{is} and floating potential V_f in the bulk plasma and near the electrode regions. Transition time T_{tr} between two states was dependent on the bulk region, and it was less than ms and ~ a few ms for I_{is} and V_f, respectively. On the other hand, T_{tr} was very small for the bias current on the order of ~ μs, and it was also small for I_{is} and V_f, which have less than a few tens of μs near the electrode region, where structural changes of plasma potential and density were observed at the transition. These showed the importance of the sheath, electrode region to trigger the transition coming from the two-dimensional particle balance and motion with sheath type instabilities.

Key words: *Plasma, Transition, Bistability, Self-excitation, Biasing, Electrode, Electric field, Magnetic field*

1. Introduction

Transition and bifurcation phenomena in plasmas have been supplying many various interesting topics in the fields of basic nonlinear physics as well as the fundamental plasma physics including fusion-oriented research. The intrinsically nonlinear characteristics of the plasma exhibit various interesting phenomena [1-19] such as the self-organized structural formation including hystereses. However, there have been few experiments [5-9] from a basic viewpoint to study these transitions.

Recently, density transitions in bistable systems were clearly found and reported [20,21], by voltage biasing to electrodes inserted into the rf-produced, cylindrical magnetized plasma: density transitions and back ones between two global states, accompanied by potential changes. Control of the staying time and staying probability in one of two states, by changing the bias voltage, was tried, with also emphasizing hysteresis characteristics in a statistical sense. Although general features of transitions were found in the previous papers [20,21], simultaneous spatio-temporal behaviors were not obtained due to the limited channels of the probes and the data acquisition system. Furthermore, the structures near the electrode have not been measured in spite of suggesting its importance of triggering transitions.

Here, we have examined spatio-temporal behaviors of global characteristics of a self-excited bistable system from a viewpoint of the transition times of parameters such as ion saturation current I_{is}, floating potential V_f, and bias current I_b, in order to have a clue of the triggering / governing mechanisms of transitions. In addition to the bulk plasma region, plasma behaviors in the sheath region (near the electrode) were investigated to understand the short transition times such as I_b, since the potential structure change in this region due to some instabilities, e.g., sheath type instabilities, is considered to initiate the transitions.

Note that these measurements have been possible due to an introduction of the new data acquisition system, multi-channel probe array, and three-dimensional moving system [22] located near the electrode.

*1 Department of Energy Engineering Science
*2 Department of Advanced Energy Engineering Science, Graduate student (Present Address: Komatsu Electronic Metals Co., Ltd.)
*3 Department of Advanced Energy Engineering Science, Graduate student (Present Address: Sharp Electronics Corp.)
*4 Research Institute for Applied Mechanics

2. Experimental Results

2.1 Experimental setup

A typical argon pressure of P_0 = 1-3 mTorr with the continuous rf power and frequency of P_{rf} = 160 W and f_{rf} = 7 MHz, respectively, were applied to a linear device, 45 cm in outer diameter and 170 cm in axial length, with the magnetic field of 500 G, as shown in Fig.1(a). Here, x (z) is taken along the radial (axial) direction. We used ten concentric rings as biased electrodes[6,7,9], and the no. 3 electrode (inner and outer radii are 3.7 and 6 cm, respectively) was used. In addition to the conventional Langmuir probes, we newly installed a 24-channel probe array, as shown in Fig.1(b), and three-dimensional probe moving system[22]. Note that the frequency responses in measuring I_{is} and V_f were more than 50 kHz and less than 10 kHz, respectively.

Most of the data were stored in the data logger with a sampling time of 10 μs. With the use of the current probe and additional logger, which has the faster sampling time of 50 ns, we could observe the fast change of I_b. For controlling the state from I to II or vice versa dynamically, a function generator and an amplifier were also used to change the bias voltage V_3.

2.2 Spatio-temporal behavior and transition time

Figure 2 shows an example of the spatio-temporal behavior as to the global change of radial I_{is} (proportional to plasma density) and V_f profiles at z = 30 cm by the 24-channel probe. Transition time T_{tr} was dependent on radial position, and there were some differences of this time between transitions from state I (I_{is} was large away from the No.3 electrode axially and in the outer radial region of this electrode) to state II (I_{is} was small in the above mentioned regions) and from state II to state I. For convenience, this time is defined as the elapsed time to take the values from 20 % to 80 % of the difference between averaged values in state I and state II.

Figure 3 shows T_{tr} of I_{is} and V_f for different axial locations, taken at x = 9 cm (in the outer radial region of the electrode). Both I_{is} and V_f

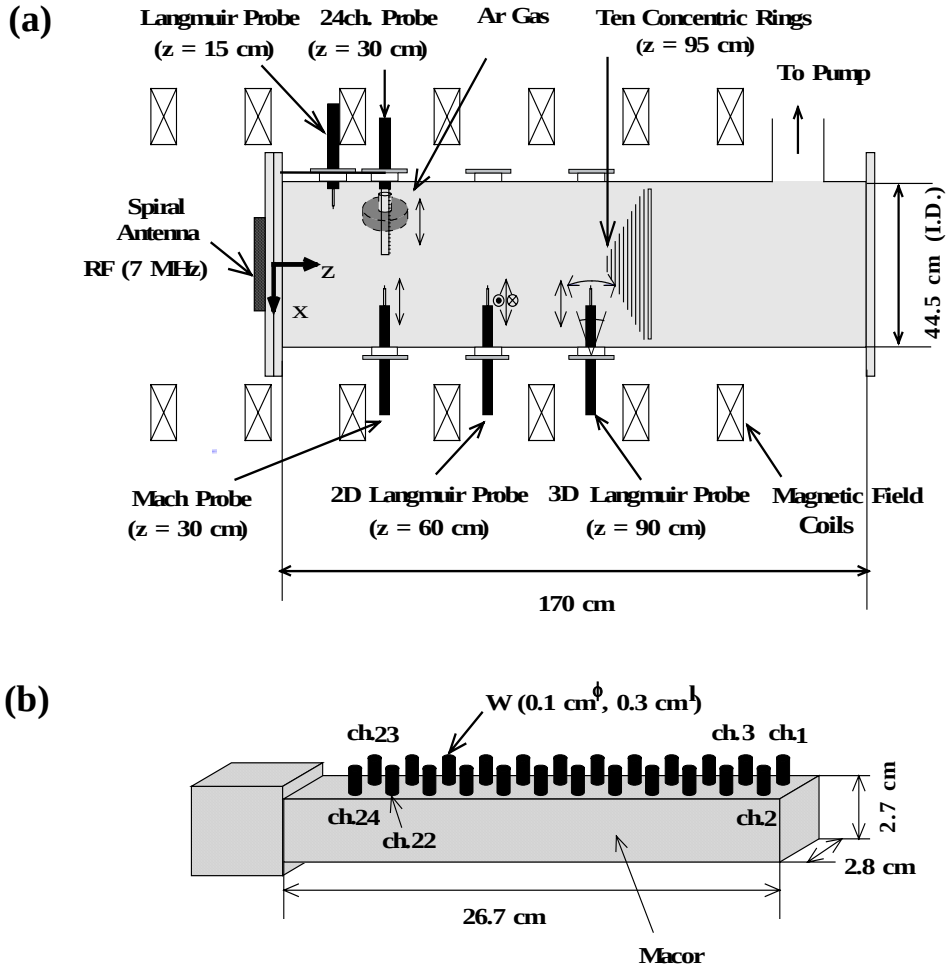

Fig.1 Schematic view of (a) experimental setup and (b) 24-channel probe array.

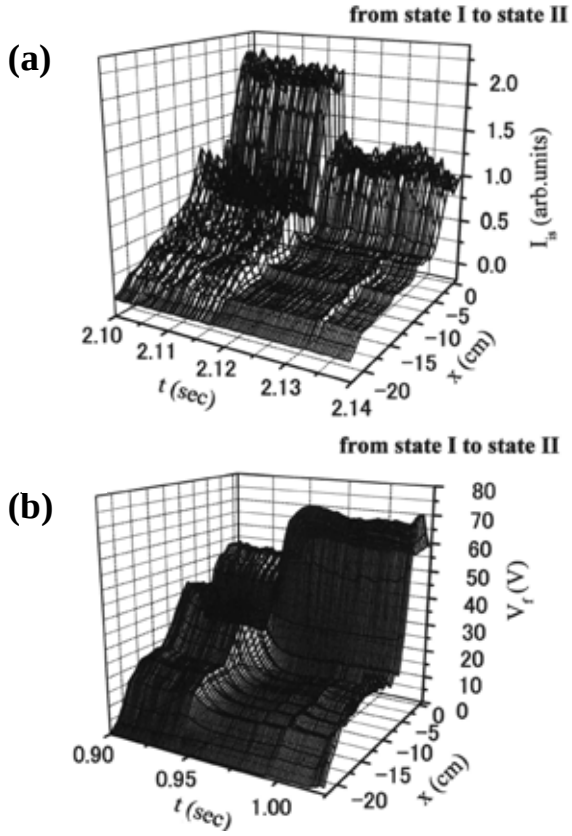

Fig.2 Spatio-temporal behaviors of (a) ion saturation current I_{is} and (b) floating potential V_f (different shots) at z = 30 cm with bias voltage V_3 = 160 V and fill pressure P_0 = 2.1 mTorr, measured by the 24-channel probe.

showed nearly constant T_{tr} regardless of the axial position. Typical T_{tr} of I_{is} was less than 0.5 ms, and T_{tr} from state I to state II is smaller than that from state II to state I (see also Fig.2). On the other hand, typical T_{tr} of V_f was on the order of a few ms, and T_{tr} from state I to state II is larger than that from state II to state I (see also Fig.2). From this, transitions occur globally at nearly the same rate regardless of the axial position.

Figure 4 shows T_{tr} of I_{is} and V_f for different radial locations, by the 24-channel probe. Different transition times depending on radial locations were found. There was a tendency that T_{tr}, for both transitions of from state I to state II and from state II to state I, was smaller in the inner radial region of the electrode than that of in the outer region in both cases of I_{is} and V_f. This may be related to the smaller plasma volume, which can change the equilibrium in the shorter time if the phenomena between the inner and outer regions are similar. Here, the case of the transition from state I to state II in I_{is} is an exception: T_{tr} was nearly constant of ~ 0.2 ms along the radial direction.

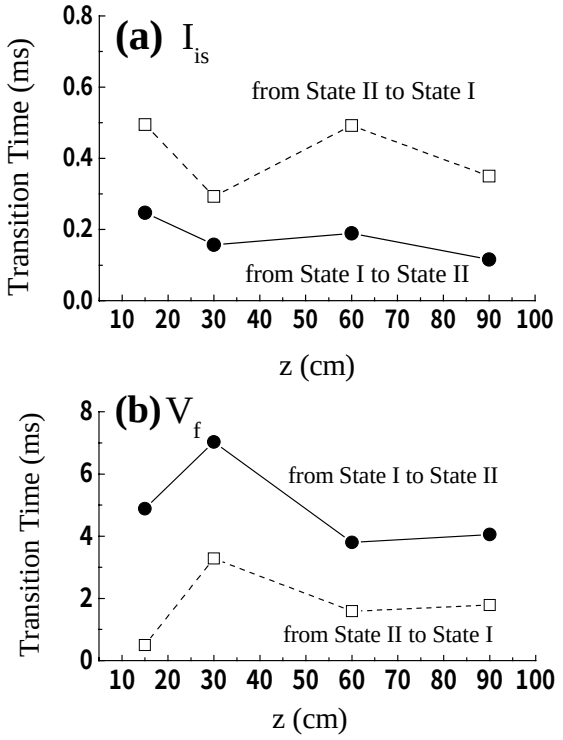

Fig.3 Transition times of (a) I_{is} and (b) V_f on different axial locations. Here, data are taken at x = 9 cm with V_3 = 157 V and P_0 = 1.8 mTorr.

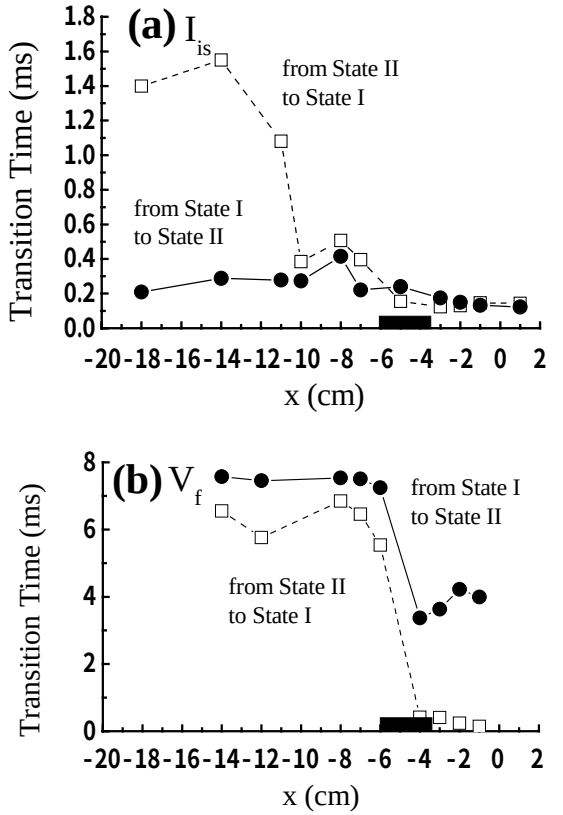

Fig.4 Transition times of (a) I_{is} and (b) V_f as a function of radial position for the same condition as that in Fig. 2. Radial position of no. 3 electrode is denoted as a horizontal closed bar.

2.3 Plasma behavior near electrode

Since the importance of the transitions near the electrode region was suggested, the spatio-temporal behaviors near this region were investigated using the scanned Langmuir probe in three-dimensional direction[22]. Figure 5 shows the spatial profiles of I_{is} and V_f in state I and state II. Mostly, this probe was moved along the arc trajectory, as shown in the inset of this figure. The probe position at θ = 12° (15.5°) corresponds to the outer radial edge of the no.2 electrode (the surface of no.3 electrode). From this, I_{is} decreased slowly (did not change so much) toward the electrode with θ = 12°-15.5° in state I (state II). This I_{is} was larger in state II than that in state I, which is the opposite behavior in the bulk plasma region, where I_{is} was larger in state I than that in state II.

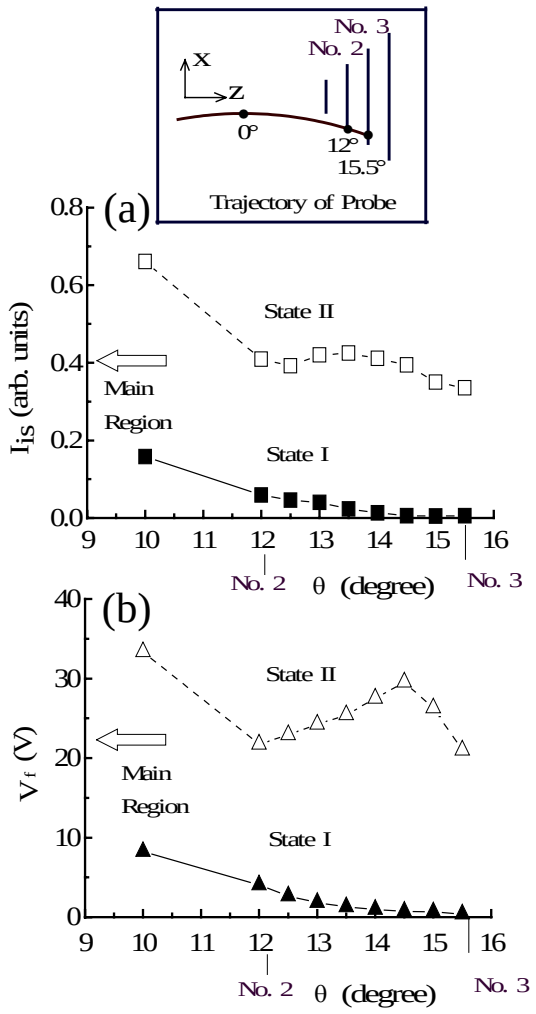

Fig.5 Spatial profiles of (a) I_{is} and (b) V_f near the electrode with V_3 = 177 V and P_0 = 1.2 mTorr. Typical values of I_{is} and V_f in the main region at the same radial location of no. 3 electrode are shown as arrows, and inset shows a trajectory of the probe.

There is a slight hump of I_{is} in state II around θ = 13.5°, which may correspond the hump of V_f (virtual anode-like) observed in Fig. 5(b). In state II, V_f was higher than that in state I by > 20 V. In state I, the value of V_f was lower than that in the central region (along the z axis) with x = 5 cm by > 15 V, which shows that the electrons can be trapped easily in the central region. This is consistent with the fact that in the bulk plasma region I_{is} in state I is larger than that in state II. On the other hand, although the sampling time of 10 μs is not enough, I_{is} near the electrode region, regardless of θ, changed very fast (< 10 μs transition time) on the same order of the changing time of I_b, which is much faster than the change of I_{is} in the bulk region. Here, T_r of V_f was also small of less than a few tens of μs (this time is limited by the measuring system mentioned before). These also show the importance of density transition near the electrode region in addition to the fast I_b change written below.

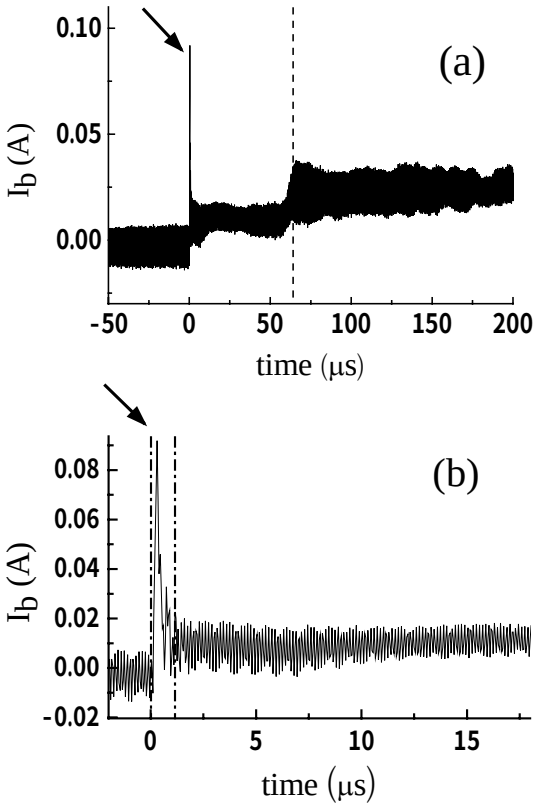

Fig.6 Time evolution of (a) I_b with P_0 = 3.5 mTorr from state I to state II by the fast rise of V_3 from 110 V to 210 V. Here, Fig. (b) shows time change of I_b of Fig. (a) in an expanding time scale.

This I_b change was carefully measured in a controlled manner. As was described, the function generator and the amplifier were used in addition to the fast logger with a sampling

time of 50 ns. Note that this does not mean the self-excited transition, but the forced transition. However, general characteristics such as the T_{tr} of I_{is} and V_f were not changed. Figure 6 shows the time evolution of I_b by the fast rise of V_3. Here, the initial (final) voltage V_3 = 110 V (210 V) corresponds to state I only (state II only). At t ~ 350 ns I_b had a sharp overshot positive spike, as is shown as an arrow in Fig.6(a), which can be clearly seen in Fig.6(b) in an expanding time scale for a different shot (there was a drift of I_b: baseline of this current, i.e. zero current, is -10 mA).

The real rise time of I_b is shorter, which is estimated to be less than several tens of ns, if considering the rise time (~ 300 ns) of V_3. Then, the fast decay (e-folding time was < 400 ns) was observed, and after t = 1.2 μs [the second chained vertical line in Fig. 6(b)], I_b became steady with some fluctuations. Here, the oscillation period of 143 ns superimposed on this I_b corresponded to the 7 MHz frequency of the rf power source. Sometimes we could see the fine different structures even in the same state of "state II", which was suggested from the distribution function of I_{is} in Ref. 21: at t = 64 μs [a vertical dotted line in Fig. 6(a)], there was the second jump of I_b and it occupied this new state steadily after that.

3. Discussion and Conclusion

The spatio-temporal characteristics of bistable system in a magnetized plasma are discussed, focusing on the triggering/governing mechanisms. This mechanism, which will be described later in detail, can be considered as follows as a promising candidate: a kind of the sheath type instabilities to change the potential structure near the electrode causes the fast change of I_b by the electron motion along the field on the order of less than several tens of ns. Next, due to the balance of the ambipolarity, ions moves slowly along the field with a time scale of the ion transit time followed by the perpendicular ion motion across the field. Final, another stable equilibrium, i.e., different, global potential and density profiles, in the bulk region is reached on a transport time scale (the ion classical transport across the magnetic field) of a few ms.

Now, detailed characteristics on transition phenomena in the initial phase are discussed. As was mentioned, the behavior near the electrode region is important, since during transitions I_b, I_{is}, and V_f changed very fast. Furthermore, there were some events with no transitions even though spikes of I_b were observed. The changing time scale of I_b was estimated to be less than several tens of ns, which is close to the characteristic time scale of the time-dependent sheath, e.g., Refs. 23 and 24, in the range of ns ($1/\omega_{pe}$ range). The decay time of I_b and the time necessary to have the steady condition after the transition for about a few μs are comparable to the ion transit time through the sheath region. The above behaviors may be related to the sheath and the ion acoustic type instabilities [25].

The next phase of transitions is considered. Due to a change of I_b, keeping the total ambipolarity leads to a change of the perpendicular ion flow due to enhanced diffusion by, e.g., change of some instabilities or turbulent states. Then, the slow change of plasma parameters in the bulk region are expected on a transport time scale. Note that the physical picture of the ion motion across the magnetic field is similar to the one in potential-driven ion cyclotron oscillations in a Q machine [26], although the time scale of ~ μs in our experiments is much shorter than the inverses of the ion cyclotron frequency of ~ 50 μs. Here, in a Q machine, the cyclotron oscillations were observed when the electrode half radius is larger than the ion Larmor radius. In our case, the transition effect fades out when the number of biased rings was increased, where the radial width of one ring was a few times of the ion Larmor radius.

In order to simulate the observed results, which suggest the sheath type instabilities, two-dimensional particle-in-cell simulations of a magnetized plasma have been carried out [27]. Preliminary results show that there is an autonomous oscillation: the main oscillation region is limited to the zone in which magnetic field lines are connected with the positively charged electrostatic plate. This is a kind of bifurcation phenomenon and appears with the potential of the plate being less than a critical value. The size of the plate must be finite across the magnetic field, because the electron and ion motions, which are mainly parallel and perpendicular to the magnetic field, respectively, influence the negative sheath facing the plate. The oscillation of the sheath width parallel to the magnetic field is synchronized with that of the amplitude of the potential, and a periodic ion bunching is also observed near the plate. The oscillation period is determined by the transit time of ions, which pass through the sheath region. These behaviors suggest a kind of two-dimensional sheath instability. This should be investigated in detail, and changing gas species may also give additional

information.

For further investigation, it is necessary to have a comparative study between experimental and stimulation results, noting the dynamic change of the two-dimensional sheath structure (local density and potential in a small area) followed by the bulk plasma one. An ion velocity distribution function may be also a key to understand this mechanism as well as the probalistic transition with hystereses[20,21].

To summarize, detailed behaviors of the self-excited bistable transition phenomena have been investigated in the bulk as well as electrode regions. Depending on the spatial region, transition time of T_{tr} was different. Near the electrode, where structural changes of the potential and the density were observed at the transition, T_{tr} was much shorter than that in the bulk region. These showed the important role of the structural changes to trigger the transitions due to the sheath type instabilities near the electrode. Next process is the ion motion along and across the field, which follows the fast change of I_b, and final, another stable equilibrium in the bulk plasma is obtained on a transport time scale.

Acknowledgments

We would like to thank Professor H. Naito for fruitful discussions and to Professor Emeritus Y. Kawai for his continuous encouragement. This work has been partly supported by the Grants-in-Aid for Scientific Research (C)(2), No.14580519, from the Japan Society for the Promotion of Science, and by the Grant-in-Aid for Encouragement of Young Researchers of the Faculty of Engineering Sciences, Kyushu University.

References

1) F. Wagner et al., Phys. Rev. Lett. **49** (1982) 1408.
2) R. J. Taylor, M. L. Brown, B. D. Frial, H. Grote, J. R. Liberati, G. J. Morales, P. Pribyl, D. Darrow, and M. Ono, Phys. Rev. Lett. **63** (1989) 2365.
3) A. Tsushima, T. Mieno, M. Oertl, R. Hatakeyama, and N. Sato, Phys. Rev. Lett. **56** (1986) 1815.
4) O. Sakai, Y. Yasaka, and R. Itatani, Phys. Rev. Lett. **70** (1993) 4071.
5) S. Shinohara, H. Tsuji, T. Yoshinaka, and Y. Kawai, Surf. Coat. Technol. **112** (1999) 20.
6) S. Shinohara, N. Matsuoka, and T. Yoshinaka, Jpn. J. Appl. Phys. **38** (1999) 4321.
7) S. Shinohara, N. Matsuoka, and S. Matsuyama, Trans. Fusion Technol. **39** (2001) 358.
8) S. Matsuyama, S. Shinohara, and O. Kaneko, Trans. Fusion Technol. **39** (2001) 362.
9) S. Shinohara, N. Matsuoka, and S. Matsuyama, Phys. Plasmas **8** (2001) 1154.
10) A. Fujisawa et al , Phys. Rev. Lett. **81** (1998) 2256.
11) P. Y. Cheung and A. Y. Wong, Phys. Rev. Lett. **59** (1987) 551.
12) J. Hopwood, Plasma Sources Sci. Technol. **1** (1992) 109.
13) F. Greiner, T. Klinger, and A. Piel, Phys. Plasmas **2** (1995) 1810.
14) T. Klinger, F. Greiner, A. Rohde, and A. Piel, Phys. Plasmas **2** (1995) 1822.
15) C. Arnas Capeau, G. Prasad, G. Bachet, and F. Doveil, Phys. Plasmas **3** (1996) 3331.
16) Y. Ping, C. X. Yu, J. L. Xie, J. Ke, X. W. Hu, H. Li, and W. X. Ding, Phys. Plasmas **8** (1996) 5006.
17) S. Shinohara, Y. Miyauchi, and Y. Kawai, Plasma Phys. Control. Fusion **37** (1995) 1015.
18) S. Takamura, M. Y. Ye, T. Kuwabara, and N. Ohno, Phys. Plasmas **5** (1998) 2151.
19) S. Shinohara and K. Yonekura, Plasma Phys. Control. Fusion **42** (2000) 41.
20) S. Matsuyama and S. Shinohara, J. Plasma Fusion Res. SERIES **4** (2002) 528.
21) S. Shinohara and S. Matsuyama, Phys. Plasmas **9** (2002) 4540.
22) S. Shinohara, Rev. Sci. Instrum. **74** (2003) 2357.
23) A. C. Calder and J. G. Laframboise, Phys. Fluids B **2** (1990) 655.
24) T–Z. Ma and R. W. Schunk, Plasma Phys. Control. Fusion **34** (1992) 767.
25) K. J. Reitzel and G. J. Morales, Phys. Plasmas **5** (1998) 3806.
26) N. Sato and R. Hatakeyama, J. Phys. Soc. Jpn. **54** (1985) 1661.
27) H. Nagahara, Y. Nakano, H. Naito, S. Shinohara, M. Yagi, and O. Fukumasa, *Proc. 7th APCPST & 17th SPSM* (Fukuoka, Japan, 2004) p. 198.